DOI: 10.1002/zaac.200700419

Synthesis and Characterization of $MoFe_3S_4$ and $Mo_2Fe_2S_4$ Single Cubanes

Markos Koutmos, Irene P. Georgakaki, Panagiotis Tsiolis and Dimitri Coucouvanis*

Ann Arbor/USA, University of Michigan

Received May 10th, 2997; accepted August 29th, 2007.

Dedicated to Professor Dieter Fenske on the Occasion of his 65th Birthday

Abstract. The synthesis of multimetallic M/S clusters by the reductive coupling of dimeric building blocks appears to be of general utility. In this paper we describe the synthesis and characterization of new single cubanes with cores such as $[Mo_2Fe_2S_4]^{2+}$ and $[MoFe_3S_4]^{3+,2+}$.

Keywords: Nitrogenase; Cluster compounds (Mo/Fe/S); Cubanes

Introduction

New crystallographic evidence of the presence of a light atom at the center of the FeMo-cofactor [1], the active site for N_2 "fixation" in nitrogenase [2], introduced a structural feature that now presents an additional challenge in the synthesis of nitrogenase-cofactor analog clusters. Unraveling the uncertainty [3] regarding the nature of this light atom, will probably involve biologists, spectroscopists and synthetic chemists. As of now synthetic efforts have not been successful in creating a synthetic analogue. These efforts are mainly centered on the synthesis and studies of single Fe/Mo/S cubanes [4] and more recently double-fused cubanes with the $Mo_2Fe_6S_8$ core [5].The later, are closer in composition with the active site structure, and potentially may undergo core rearrangements to structures close to that of the FeMo-cofactor.

A rational synthetic pathway to FeMoS clusters, developed in our laboratories, involves the reductive coupling of Fe_2S_2 and $MoFeS_2$ dimers in the presence of trialkyl phosphines [6]. A number of single $MoFe_3S_4$ cubanes as well as the double-fused cubanes $Mo_2Fe_6S_8$ have been synthesized based on this methodology, and include $[(Cl_4cat)(L)MoFe_3S_4Cl_3]^{2-}$, $[(Cl_4cat)(L)Mo_2Fe_2S_3O\ (PEt_3)_3Cl]^{2-}$ (L = THF, CH_3CN) and $(Cl_4cat)_2Mo_2Fe_6S_8(PR_3)_6$ (R = Et, Bu, Pr). In this paper we describe the synthesis and characterization of four new single cubanes, $(Cl_4\text{-cat})(py)MoFe_3S_4(PCy_3)_3$, (**I**) $(Cl_4\text{-cat})(THF)MoFe_3S_4(PMe^tBu_2)_3$, (**II**) $(Cl_4\text{-cat})(PTA)MoFe_3S_4Cl_3[Fe(DMF)_5]$ (PTA = 1,3,5 triaza-7phosphaadamantane), (**III**) and $(Cl_4\text{-cat})_2Mo_2Fe_2S_4(PPr_3)_4$, (**IV**).

* Prof. Dimitri Coucouvanis
University of Michigan
930 N. University,
Ann Arbor, MI 48109 / USA
Fax: ++ (734) 936 2916
E-mail: dcouc@umich.edu

Experimental Section

General

All experiments and reactions were carried out under a dinitrogen atmosphere using standard Schlenk line techniques or in an inert atmosphere glove box.All solvents were distilled under dinitrogen and nitrogen gas was bubbled through each before use in the glove box. Acetonitrile was pre-dried over oven-dried molecular sieves and distilled over CaH_2. Ethyl ether and THF were pre-dried over Na ribbon and further purified by the Sodium-Benzoketyl method. Dichloromethane was distilled over CaH_2. Tetrachlorocatechol (Cl_4-catH_2) (Lancaster) was dissolved in ethyl ether and the concentrated solution was treated with activated charcoal (Aldrich). After a few hours, the mixture was filtered by gravity filtration and the process continued until the ether solution contained no dark brown color. Once the color of the diethyl ether solution became lighter, the solvent was removed by nitrogen purging and the residue was dried under vacuum. Anhydrous $FeCl_2$, P^nPr_3, PCy_3, PMe^tBu_2, $NaPF_6$, and $NaBPh_4$ were purchased from STREM or Aldrich and used without further purification. $(NH_4)_2[MoO_2S_2]$ [7], $(Et_4N)_2[FeCl_4]$ [8], $(Et_4N)[FeCl_4]$, $(Et_4N)_2[Fe_2S_2Cl_4]$ [9] and pta (1,3,5 triaza-7phospha-adamantane) [10] were synthesized according to published methods after slight modifications.

FT-IR spectra were collected on a Nicolet DX V. 4.56 FT-IR spectrometer in KBr pellets and the spectra were corrected for background. Elemental analyses were performed by the Microanalytical Laboratory at the University of Michigan. The data were corrected using acetanilide as a standard. Electronic spectra were recorded on a Varian CARY 1E UV-Visible spectrometer. Allcyclic voltammetry experiments were carried out with glass working and Ag/AgCl reference electrode with 0.1M of Bu_4NPF_6 supporting electrolyte in a EG&G Princeton potentiostat/galvanostat Model 263A. The redox potentials were reported vs SCE. ((rev),reversible; (qr), quasi-reversible; (irr), irreversible).

The compounds of primary interest are designated as follows:

$(Cl_4\text{-cat})(py)MoFe_3S_4(PCy_3)_3$	**I**
$(Cl_4\text{-cat})(THF)MoFe_3S_4(PMe^tBu_2)_3$	**II**
$[(Cl_4\text{-cat})(PTA)MoFe_3S_4Cl_3][Fe(DMF)_5]$	**III**
$[(Cl_4\text{-cat})_2(P^nPr_3)_2Mo_2Fe_2S_4(P^nPr_3)_2)]$	**IV**

$(Cl_4\text{-cat})(pyr)MoFe_3S_4(PCy_3)_3$ (I)

0.75 g (0.93 mmol) of $(Et_4N)_2[(Cl_4\text{-cat})MoOS_2FeCl_2]$ were dissolved in ~ 30 ml of acetonitrile followed by the addition of 0.49 g of $(Et_4N)_2[Fe_2S_2Cl_4]$. 1.18 g of $P(C_6H_{11})_3$ were dissolved in 5 ml of pyridine and were subsequently added via a syringe to the acetonitrile mixture dropwise and under vigorous stirring. 0.94 g (5.58 mmol) of $NaPF_6$ were then added. The reaction mixture was stirred for 2 days. The precipitate that formed was collected via filtration through a fritted funnel with celite, and was washed thoroughly with acetonitrile, methanol and hexanes. The black solid was then dissolved in 25 ml of CH_2Cl_2 and layered with hexanes. 500 mg of crystalline material were isolated (35 % yield). Crystals of the product, suitable for X-Ray structure determination, were obtained from an ether solution of this compound, through slow evaporation of the solvent. Black rhombic crystals isolated were suitable for X-Ray determination. Analysis. Calculated for $MoFe_3O_2P_3S_4Cl_4C_{65}H_{104}$ (**I**). (MW 1557.42): C, 50.09; H, 6.73.; N, 0.90 Found: C, 50.74; H, 6.95; N, 0.74 %.

FT-IR (KBr, cm^{-1}) 3004(w), 2961(m), 2925(m), 2860(m), 1481(m), 1431(vs), 1391(m), 1375(m), 1283(w), 1255(s), 1217(m), 1183(m), 1170(m), 1098(m), 1062(m), 1030(m), 1000(m), 978(s), 839(s), 807(s), 781(s), 695(m), 630(w), 558(m), 541(m), 441(w), 425(m), 411(m).

$[(Cl_4\text{-cat})(THF)MoFe_3S_4(PMe^tBu_2)_3]$ (II)

The same procedure (see above) as for cluster **I** was used with 0.55 g (0.68 mmol) of $(Et_4N)_2[(Cl_4\text{-cat})MoOS_2FeCl_2]$, 0.37 g (0.68 mmol) of $(Et_4N)_2[Fe_2S_2Cl_4]$, 0.5 g (0.9 ml, 3.11 mmol) of PMe^tBu_2 in 12 ml of acetonitrile, and 0.63 g (3.78 mmol) of $NaPF_6$ in 20 ml of MeCN. A black-colored powder was isolated after filtration and thorough washing with acetonitrile, methanol, and hexanes. The compound was recrystallized from dichloromethane and hexanes to afford 200 mg (27 % yield) of the product. Black crystals that were isolated were suitable for X-Ray determination. Analysis. Calculated for $MoFe_3O_3P_3S_4Cl_4C_{37}H_{67}$, (**II**), (MW 1186.30): C, 37.45; H, 5.69. Found: C, 37.74; H, 5.84 %.

$[(Cl_4\text{-cat})(PTA)MoFe_3S_4Cl_3][Fe(DMF)_5]$ (III)

1.5 g (1.85 mmol) of $(Et_4N)_2[(Cl_4\text{-cat})OMoS_2FeCl_2]$ and 1 g (1.73 mmol) of $(Et_4N)_2[Fe_2S_2Cl_4]$ were dissolved in 20 ml of acetonitrile followed by the addition of 0.58 g (3.70 mmol) of PTA, and 0.93 g (5.55 mmol) of $NaPF_6$. The reaction was stirred 2 days before it was filtered. The precipitate was washed thoroughly with acetonitrile, methanol, THF and ether. Most of the resulting material was extracted with 75 ml of DMF. Black colored powder of $[(Cl_4\text{-cat})(pta)MoFe_3S_4Cl_3][Fe(DMF)_5]$ (**III**). (350 mg, 10.8 % yield) was isolated after filtration. Black crystals were obtained from slow diffusion of ether to a DMF solution of compound **III**. Analysis. Calculated for $MoFe_4O_7PS_4Cl_7N_8C_{27}H_{52}$ (**III**), (MW 1327.48): C, 24.43; H, 3.95; N, 8.44. Found: C, 24.98; H, 4.14; N, 9.12 %.

$(Cl_4\text{-cat})_2Mo_2Fe_2S_4(P^nPr_3)_4$ (IV)

To a solution of $(Et_4N)_2[(Cl_4\text{-cat})OMoS_2FeCl_2]$ (1.1 g, 1.36 mmol) and $(Et_4N)_2[Fe_2S_2Cl_4]$ (0.72 g, 1.25 mmol) in 30 mL CH_3CN, P^nPr_3 (1.9 mL, 9.2 mmol) was added dropwise via a syringe while stirring. A solution of $NaPF_6$ (1.4 g, 8.3 mmol) in 5 mL CH_3CN was then added followed by the addition of Bu_4NOH (2.7 mL 1M THF solution, 2.7 mmol). The reaction mixture was stirred overnight at room temperature and then filtered through celite. The solvent was pulled off in the filtrate using N_2 stream leaving a black solid which was washed with MeOH and dissolved in Et_2O. Slow evaporation of Et_2O afforded the product as black needle-shaped crystals suitable for x-ray structure determination.

IR (KBr, cm^{-1}): 2962(s), 2931(m), 2871(m), 1435(s), 1378(m), 1288(w), 1252(s), 1087(s), 976(s), 904(w), 807(s), 779(ms), 530(m).

X-ray crystallography

All diffraction data were collected at the University of Michigan X-Ray facility, at low temperatures ranging from 123(2) to 158(2) K to avoid crystal decay during data collection, using a SIEMENS SMART area X-ray diffractometer equipped with an LT-2 low temperature device and normal focus Mo-target X-ray tube ($\lambda\lambda$ = 0.71073 Å). All diffraction data were processed with SADABS for absorption correction [11]. The positions of heavy atoms were found by direct methods in E-maps using the software solution program in SHELXTL v.6.1 [12]. Subsequent cycles of least-squares refinement followed by difference Fourier synthesis produced the positions of the remaining non-hydrogen atoms; which were refined anisotropically unless stated otherwise. All hydrogen atoms were placed in ideal positions and refined as riding atoms with individual (or group if appropriate) isotropic thermal displacement parameters. The crystal data and structural parameters are shown in Table 1. All space group assignments were determined based on systematic absences and intensity statistics and were confirmed by the program XPREP of the SHELXTL package.

The space groups for clusters **I, II, III, and IV** are $P2_1/c$ (monoclinic), $P2_12_12_1$ (orthorhombic), $P\bar{1}$ (triclinic), and $C2/c$ (monoclinic), respectively. In cluster **II** the solvent molecule (THF) bound to the Mo atom is disordered. In **III** The C atoms (C1, C4, C5, C8, C9, and C10) as well as the N atoms (N1 (PTA ligand), N2, and N6 (DMF ligands)) were treated isotropically. **III** crystalizes with DMF solvent molecule in the lattice (one molecule in the asymmetric unit). In **IV** the phosphine ligand bound on Fe(1) as well as the phosphine C atoms (64, 65, 68, 69) are disordered. Refinement was performed after modeling these atoms in two different sites (positions) and employing command *Part*. Highly disordered ether molecules also are found in the crystal lattice of **IV**. Full matrix least-squares refinement based on F2 converged to R1 values of 0.0387, 0.0702, 0.0500 and 0.0596 and a wR2 value of 0.0985, 0.1682, 0.0992, and 0.1556 for **I, II, III and IV,** respectively. Ortep diagrams for **I, II, III and IV** are provided in figures 1, 2, 3 and 4, respectively.

Results and Discussion

$(Cl_4\text{-cat})(py)MoFe_3S_4(PCy_3)_3$ (I), $(Cl_4\text{-cat})(THF)MoFe_3S_4(PMe^tBu_2)_3$ (II)

The effect of phosphine ligand cone angles in the synthesis of high nuclearity Mo/Fe/S clusters as discussed previously [5b, 6] is also evident in the formation of clusters **I** and **II**. When bulky phosphine ligands such as PCy_3, and PMe^tBu_2 with cone angles of 170° and 145° respectively [13], are used instead of PR_3 (R: Et, ^{n}Pr, or ^{n}Bu), (in reductive coupling syntheses), single cubanes with the $[MoFe_3S_4]^{2+}$ cores form. Double-fused cubanes with $(Mo_2Fe_6S_8)$ cores and $[MoFe_3S_4]^{2+}$ subunits form with less bulky phosphines. The double-fused cubane clusters,

Table 1 Crystallographic and refinement data for $(Cl_4\text{-cat})(pyr)MoFe_3S_4(PCy_3)_3$ (**I**), $(Cl_4\text{-cat})(THF)MoFe_3S_4(PMe^tBu_2)_3$ (**II**), $[(Cl_4\text{-cat})(PTA)MoFe_3S_4Cl_3][Fe(DMF)_5]$ (**III**), $[(Cl_4\text{-cat})_2(P^nPr_3)_2Mo_2Fe_2S_4(P^nPr_3)_2)]$ (**IV**).

Compound	I	II	III	IV
empirical formula	$C_{65}H_{104}Cl_4Fe_3MoNO_2P_3S_4$	$C_{38}H_{63}Cl_4Fe_3MoO_3P_3S_4$	$C_{35}H_{50}Cl_7Fe_4MoN_9O_8PS_4$	$C_{48}Cl_8Fe_2Mo_2O_6P_4S_4$
formula weight	1557.93	1194.32	1451.90	1564.29
crystal system	monoclinic	orthorhombic	triclinic	monoclinic
space group	$P2_1/c$	$P2_12_12_1$	$P\bar{1}$	$C2/c$
a, Å	12.921(3)	11.1008(8)	10.754(4)	40.648(10)
b, Å	22.446(5)	12.4407(9)	12.362(4)	20.242(5)
c, Å	25.633(5)	38.761(3)	21.086(7)	18.296(4)
α, deg	90.00	90	84.257(6)	90
β, deg	103.65(3)	90	76.848(5)	93.101
γ, deg	90.00	90	74.699(6)	90
V, Å^3	7224(3)	5352.9(7)	2630.6(15)	15032(6)
density, mg/mm^3	4, 1.432	4, 1.482	2, 1.833	8, 2.251
temperature, K	153(2)	153(2)	150(2)	123(2)
absorption coeff, mm^{-1}	1.132	1.503	1.909	2.990
F(000)	3256	2448	1462	9706
crystal size, mm	N/A	N/A	0.34 x 0.04 x 0.03	0.34 x 0.24 x 0.06
θ range for data colln, deg	2.69 to 28.32	1.72 to 27.54	1.94 to 18.08	2.84 to 24.85
limiting indices	$-21 < h < 20$	$-14 < h < 14$	$-9 < h < 9$	$-47 < h 47$
	$-28 < k < 30$	$-16 < k < 16$	$-10 < k < 10$	$-23 < k < 23$
	$-36 < l < 36$	$-50 < l < 49$	$-18 < l < 18$	$-21 < l < 21$
R(int)	0.000	0.0422	0.1175	0.0936
completeness to θ, %	99.4	99.6	98.8	99.1
reflections collected	17900	12208	10694	12896
data/restraints/parameters	17900 / 0 / 723	12208 / 0 / 501	3626 / 0 / 603	12896 / 0 / 767
final R indices [$I > 2\sigma(I)$], R1, wR2	0.0387, 0.0985	0.0702, 0.1682	0.0500, 0.0992	0.0596, 0.1556
R indices (all data), R1, wR2	0.0468, 0.1035	0.0839, 0.1753	0.1252, 0.1295	0.1039, 0.1819
goodness-of-fit on F^2	1.086	1.103	0.983	1.038

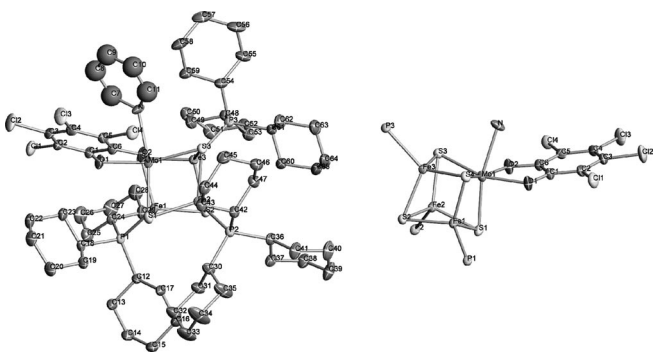

Figure 1 ORTEP diagrams of the $(Cl_4\text{-cat})(py)MoFe_3S_4(PCy_3)_3$ (**I**) core showing the thermal ellipsoids at 50 % probability. On the left hydrogen atoms of the phosphine ligands have been omitted. On the right both the carbon and the hydrogen atoms of the phosphine groups as well as of the solvent (pyridine) ligand have been omitted for clarity.

$[(Cl_4\text{-cat})_2Mo_2Fe_6S_8(PEt_3)_6]$, form when two single cubanes with the $[MoFe_3S_4]^{3+}$ core undergo reduction with concomitant phosphine binding at the molybdenum and iron sites.Cluster fusion and edge Fe−S bridging lead to the double cubane arrangement. Phosphines with large cone angles, such as PCy_3 or PMe^tBu_2, are sterically encumbered and do not bind to the octahedral Mo site which instead binds to a solvent molecule (pyridine in **I** or THF in **II**). The smaller cone angles of PR_3 (R: Et, ^{n}Pr, or ^{n}Bu) allows edge fusion and Mo binding in the $[(Cl_4\text{-cat})_2Mo_2Fe_6S_8(PEt_3)_6]$ clusters.

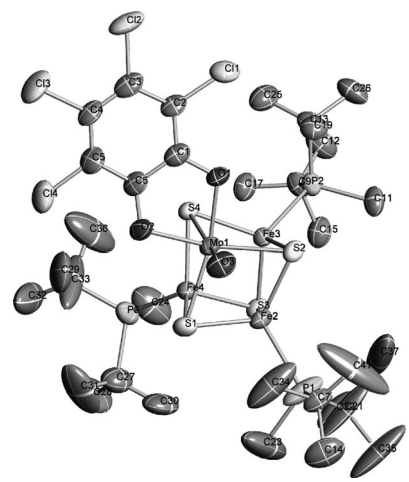

Figure 2 ORTEP diagram of the $(Cl_4\text{-cat})(THF)MoFe_3S_4(PMe^tBu_2)_3$ (**II**) cluster showing the thermal ellipsoids at 50 % probability. The hydrogen atoms of the phosphine ligands as well as the carbon and hydrogen atoms of the solvent (THF) of the ligand have been omitted.

The $[MoFe_3S_4]^{2+}$ single cubane core with phoshines as terminal ligands is not unprecedented. Clusters with such a core have been reported by *Holm* et al. [5b] and have been obtained through the "traditional" route from the reaction of cluster $(Et_4N)_2[(Cl_4\text{-cat})(MeCN)MoFe_3S_4Cl_3]$ with excess of bulky phosphines such as P^iPr_3 and P^tBu_3 and $NaBPh_4$.

The reactivity of clusters **I** and **II**, and especially that of cluster **I** were investigated under reductive conditions. Cyc-

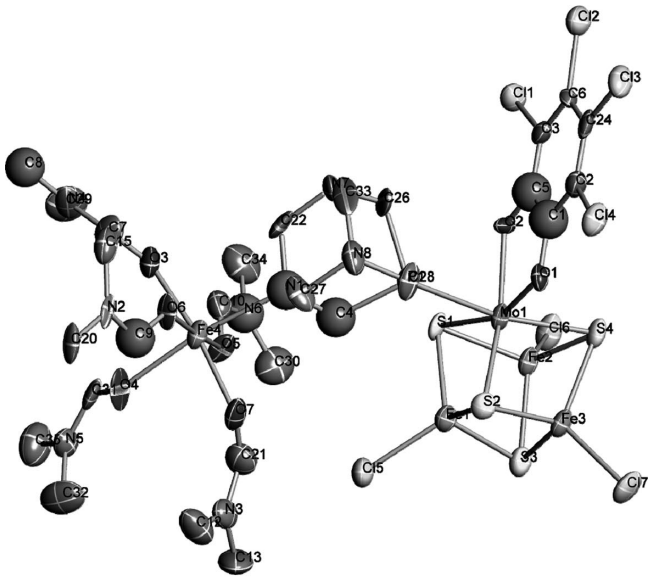

A

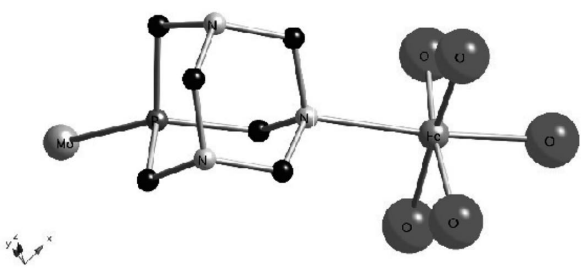

B

Figure 3 Ortep diagram of **A** the $[(Cl_4\text{-cat})(PTA)MoFe_3S_4Cl_3]$-$[Fe(DMF)_5]$ (**III**) cluster showing the thermal ellipsoids at 50 % probability. The hydrogen atoms of the phosphine and the DMF ligands have been omitted for clarity. **B**, the PTA bridge.

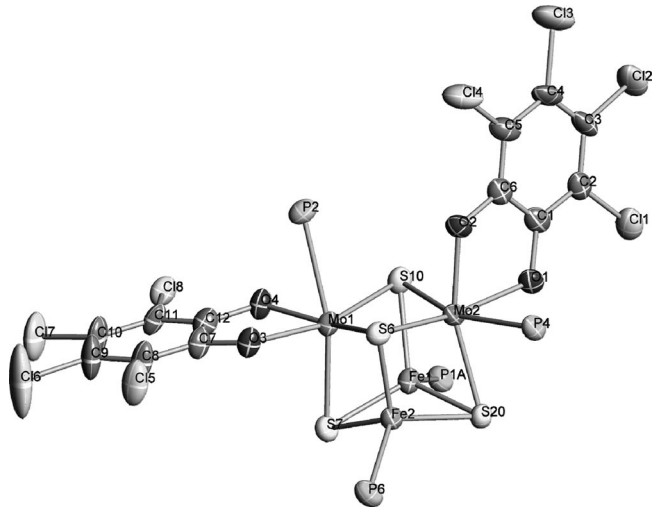

Figure 4 Ortep diagram of the $[(Cl_4\text{-cat})_2(P^nPr_3)_2Mo_2Fe_2S_4(P^nPr_3)_2)]$ **IV** cluster showing the thermal ellipsoids at 50 % probability. The carbon and hydrogen atoms of the phosphine ligands have been omitted for clarity.

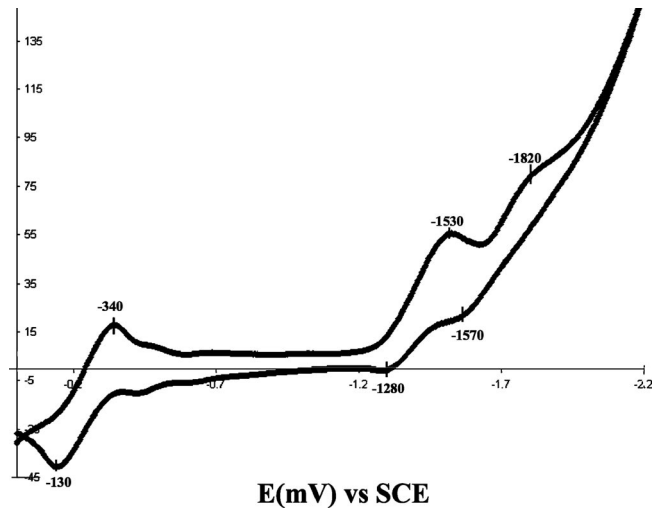

Figure 5 Cyclic voltammogram in THF demonstrating the three-member electron transfer series of $(Cl_4\text{-cat})(pyr)MoFe_3S_4(PCy_3)_3$ (**I**); peak potentials vs SCE are indicated.

lic voltammetry of **I** (figure 5) in THF revealed three reversible reductions at −185, −1405 and −1695 mV. It appears that the first reduction under electrochemical conditions is quite facile, thus a rather mild reducing agent should achieve the one e^- reduction of **I**. Unfortunately, no chemical reduction could be achieved even with strong reducing agents such as potassium anthracenide. Moreover, the reactivity of **I** was explored under the reductive conditions of a carbon monoxide (CO) atmosphere. It was of interest to see if "Roussin" like products with the $MoFe_3S_3$ core structure could be obtained [14]. Under 500 psi CO pressure a mixture of compounds formed that required the use of column chromatography for their separation. The isolated material differed form the sulfur voided cubanes [14] as evident by differences (CO region) in the IR spectra. Single crystal X-Ray structural determination of the major product revealed the $(THF)_3COMo(\mu_3\text{-}S)Fe_2(CO_6)$ structure (see supporting information). When lower pressures of CO were applied (∼150 psi) the starting material was isolated indicating that no reaction had taken place.

$[(Cl_4\text{-cat})(PTA)MoFe_3S_4Cl_3][Fe(DMF)_5]$(III)

The synthesis of cluster **III** was achieved employing a similar synthetic strategy with the one used for the $[(Cl_4\text{-cat})_2$-

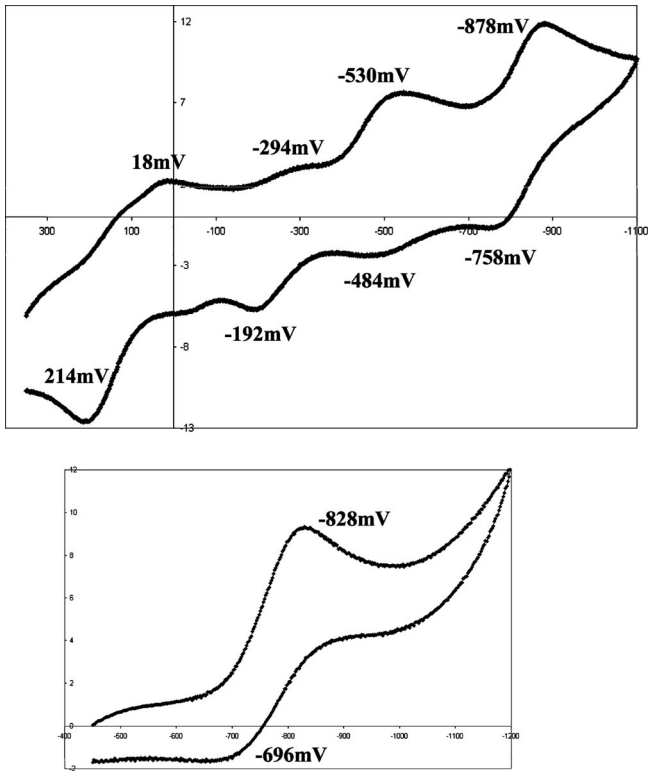

Figure 6 Cyclic voltammograms of clusters $[(Cl_4\text{-cat})_2(P^nPr_3)_2\text{-}Mo_2Fe_2S_4(P^nPr_3)_2)]$ (**IV**), in THF (top) and $[(Cl_4\text{-cat})(pta)\text{-}MoFe_3S_4Cl_3][Fe(DMF)_5]$ (**III**), in acetonitrile (bottom); peak potentials vs SCE are indicated..))

$Mo_2Fe_6S_8(PEt_3)_6$ clusters [5]. The only modification was the use of 2 eq of PTA instead of 1 eq of PEt_3. Our intention initially was to synthesize a cluster that would have the same structure as the $[(Cl_4\text{-cat})_2Mo_2Fe_6S_8(PR_3)_6]$ clusters but with PTA ligands (figure 3) instead of PR_3 (R: Et, ^{n}Pr, or ^{n}Bu) The PTA ligand is easy to make and rather inexpensive and can be obtained in multigram quantities.Moreover it is water soluble and it would allow us to investigate the chemistry of clusters with the composition and structure similar to $[(Cl_4\text{-cat})_2Mo_2Fe_6S_8(PR_3)_6]$ in different solvents and more importantly in the presence of water as reactant or potential ligand.The presence of basic N sites in the PTA ligand also could facilitate the delivery and uptake of H^+ by the Mo_2Fe_6 complexes. All these attributes urged us to pursue the synthesis of $Mo_2Fe_6S_8$ clusters with the PTA ligands.

It is worthwhile noticing that the reaction of $(Et_4N)_2[(Cl_4\text{-cat})MoOFeS_2Cl_2]$ and $(Et_4N)_2[Fe_2S_2Cl_4]$ with PTA and $NaPF_6$, in stoichiometries analogous to the ones that lead to the formation of $[(Cl_4\text{-cat})_2Mo_2Fe_6S_8(PR_3)_6]$ clusters, eventually resulted in the isolation again of compound **III**. In all cases the original precipitate of the reaction mixture was insoluble in all solvents except DMF. It is clear that this precipitate is not the same as cluster **III** (based on IR and elemental analysis) but somehow DMF promotes the formation of **III**. Cluster **III** exhibits a reversible reduction wave at −762 mV (figure 6) and two irreversible oxidations at 586 mV and 916 mV. The reduction potential is comparable to the corresponding ones of other $MoFe_3S_4$ single cubanes that range from 0.83 to 1.31 mV [15], albeit somewhat lower.

$[(Cl_4\text{-cat})_2(P^nPr_3)_2Mo_2Fe_2S_4(P^nPr_3)_2)]$ (IV)

Among the large number of cuboidal Mo/Fe/S clusters that have been reported [16], clusters with the $[Mo_2Fe_2S_4]$ core are not very common.Known clusters with the $[Mo_2Fe_2S_4]$ cores include: a) the $Mo_2Fe_2S_4(S_2CNEt_2)_5$ cluster obtained through a self-assembly reaction [17] and b) the structurally characterized organometallic clusters, $(Me_5C_5)_2Mo_2Fe_2S_4Cl_2$ [18], $Mo_2Fe_2S_4(C_5EtMe_4)_2(NO)_2$ [19] and $Mo_2Fe_2S_4\text{-}(C_5Me_5)_2(CO)_4$ [20]. These were obtained by condensation of $RMoX_n$ or $R_2Mo_2S_4X_n$ blocks (R = Cp or its derivatives, X = terminal ligand) and various ironsources ($FeCl_3$, $Na[Fe(CO)_3(NO)]$, $Fe_2(CO)_9$).

The reductive coupling of the $[(Cl_4\text{-cat})Mo(O)S_2FeCl_2]^{2-}$ dimer was previously carried out using $Fe(PEt_3)_2Cl_2$ as a reducing and chloride scavenging agent, and resulted in the formation of the $(Cl_4\text{-cat})_2Mo_2Fe_2S_3O(PEt_3)_3Cl]\cdot 1/2(Fe(PEt_3)_2\text{-}(MeCN)_4$ (**V**) salt, with an anionic cluster containing the hitherto unknown $[Mo_2Fe_2S_3O]$ core.

The versatility of the $Fe(PEt_3)_2Cl_2$ iron reagent has been demonstrated previously in the syntheses of the $(Cl_4\text{-cat})_2\text{-}Mo_2Fe_6S_8(PR_3)_6$ (R = Et, ^{n}Pr) and $Fe_6S_6(PEt_3)_4Cl_2$.In the synthesis of $(Cl_4\text{-cat})_2Mo_2Fe_2S_3O(PEt_3)_3Cl]\cdot 1/2(Fe(PEt_3)_2\text{-}(MeCN)_4$, the PEt_3 from $Fe(PEt_3)_2Cl_2$ abstracts S or O atoms from $(Et_4N)_2[(Cl_4\text{-cat})MoOS_2FeCl_2]$ with formation of $SPEt_3$ or $OPEt_3$. Following reduction and ligand substitution (Cl^- by $\mu\text{-}S^{2-}$), the Mo/Fe dimers undergo coupling and produce the $[Mo_2Fe_2S_3O]$ cuboidal cluster. The previous isolation [6] of the $[Mo_2Fe_2S_3O]$ cluster but not of the $[Mo_2Fe_2S_4]$ or $[Mo_2Fe_2S_2O_2]$ clusters is perhaps fortuitous and intriguing.

Slight modifications in the synthesis of cluster $[(Cl_4\text{-cat})_2\text{-}Mo_2Fe_6S_8(PPr_3)_6]$, resulted in the reproducible formation of a new compound that after isolation and characterization proved to be a cluster with the $[Mo_2Fe_2S_4]^{4+}$ core. Cluster $[(Cl_4\text{-cat})_2(P^nPr_3)_2Mo_2Fe_2S_4(P^nPr_3)_2)]$ most probably assembles in the same manner as cluster $(Cl_4\text{-cat})_2Mo_2Fe_2S_3O(PEt_3)_3Cl]\cdot 1/2(Fe(PEt_3)_2(MeCN)_4$, but in the presence of more phosphine and Cl^- scavenger ($NaPF_6$) the formation of the neutral species is favored rather than the ionic one with a phosphine inplace of the Cl^- ligand.

Cyclic voltammetry for compound **IV** shows reversible reduction waves at −243, −507, and −818 mV and a reversible oxidation wave at 116 mV. In **V**, with the $MoOS_3Fe_4$ core, certain differences are apparent. The latter also exhibits three reductions waves but these are irreversible and shifted towards higher potentials (−882, −1140, and −1840 mV).It also exhibits an irreversible oxidation at 412 mV.

Structural Description

$(Cl_4$-cat)(pyr)$MoFe_3S_4(PCy_3)_3$ (I), $(Cl_4$-cat)(THF)$MoFe_3S_4(PMetBu_2)_3$ (II)

The Mo atom in both **I** and **II** is octahedrally coordinated with O_2S_3N, and O_3S_3 coordination spheres respectively. It is bound to a cathecolate ligand, three μ_3-S^{2-} ligands and one solvent molecule, (a pyridine molecule in cluster **I** with a Mo−N bond length of 2.301(2) Å, and a tetrahydrofuran molecule in **II** with a Mo−O bond length of 2.265(6) Å).The mean Mo−O and Mo−S bond distances in **I** and **II** are observed at 2.099(2,15), 2.359(2.10) Å andat 2.105(2,26), 2.364(3,9) Å respectively. The Fe atoms exhibit a distorted tetrahedral (FeS_3P) geometry with a range of S−Fe−P angles of 99.42°−120.68°, and 107.43°−116.68° for **I** and **II**, respectively. The mean Fe−S bond lengths are 2.258(9,10) and 2.254(9,6) Å, whereas the mean Fe−P distances are 2.370 Å (range: 2.312−2.403 Å), and 2.367 Å (range: 2.343−2.387 Å) respectively.

The mean Fe−Fe distances are found at 2.618(3,20) Å and at 2.614(3.3) Å in **I** and **II**, respectively, while the mean Mo−Fe distances are found at 2.675(3,9) Å and 2.670(3,5) Å, respectively. A comparison of these distances in the single cubanes with the $[MoFe_3S_4]^{2+}$ core, with corresponding distances in the $MoFe_3S_4$ subunits of the double-fused cubanes, does not show significant differences.

$[(Cl_4$-cat)(pta)$MoFe_3S_4Cl_3][Fe(DMF)_5]$ (III)

Cluster **III** is a single $[(Cl_4$-cat)$MoFe_3S_4Cl_3]^{2-}$ cubane that is connected to an Fe monomer through the pta ligand. The pta ligand is bound to the single cubane through the P and exhibits a Mo−P bond distance of 2.561(5) Å and to the Fe through the N(1) with a Fe(4)−N(1) bond length of 2.258(12) Å. The Fe ion has a distorted octahedral arrangement and its coordination is completed by five, oxygen bound,DMF ligands. The mean Fe−O bond length at 2.100(22) Å is typical for octahedral Fe in 2+ oxidation state, and renders the single cubane's core as $[MoFe_3S_4]^{3+}$. The M−M and M−S distances in the $MoFe_3S_4Cl_3$ cores at other oxidation levels are not that much different.

$[(Cl_4$-cat$)_2(P^nPr_3)_2Mo_2Fe_2S_4(P^nPr_3)_2)]$ (IV)

The overall structural features of the $[Mo_2Fe_2S_4]^{4+}$ core in **IV** are similar to those found in other $[Mo_2Fe_2S_4]$ distorted cubanes and to the $[Mo_2Fe_2S_3O]^{4+}$ core of cluster $(Cl_4$-cat$)_2Mo_2Fe_2S_3O(PEt_3)_3Cl]\cdot 1/2(Fe(PEt_3)_2(MeCN)_4$ (**V**) [6].The main difference between **IV** and **V** is the arrangement of the ligands around the Mo atom.In both clusters the Mo atoms have a distorted octahedral (MoO_2S_3P or MoO_3S_2P) environment with mean Mo−S and Mo−P bond lengths at 2.376(6,13) Å, 2.596(2,21) Å, and 2.364(4,3) Å, 2.585(2,1) Å for **IV** and **V**, respectively. In **V** the Cl_4-cat ligands have a *syn* orientation and the P ligands also havea *syn* orientation and are parallel to the plane defined by the 2Mo atoms and the the S atom in the Mo_2SO dimeric subunit.They both are *trans* to the μ_3-bridging oxygen atom. In **IV** (Fig. 4) one of the phosphine ligands is almost parallel to the plane defined by the 2Mo atoms and a S atom of the Mo_2S_2 subunit while the other phosphine ligand is almost vertical to this plane. Moreover one of the Cl-$_4$cat ligands has an almost vertical arrangement with respect to this plane while the other Cl_4-cat ligand is almost coplanar.

In **IV** the Fe atoms are in distorted tetrahedral (FeS_3P) environment with a range of 101.23°−121.85° in the P−Fe−S angles, and a mean Fe−S bond length of 2.220(6,3) Å. The Mo−Mo, Fe−Fe, distances can be found at 2.784(5) Å, and 2.601(5) Å, respectively, while the Mo−Fe distances range from 2.601(5) to 2.682(5)Å. In **V**, the corresponding M−M distances (Mo−Mo = 2.660(1) Å, Fe−Fe = 2.679(1) Å. The pronounced differencesin the Mo−Mo and Fe−Fe distances are likely attributed to the presence of bridging heteroatom (μ_3-O) in $[Mo_2Fe_2S_3O]$ rather thana μ_3-S in the $[Mo_2Fe_2S_4]$ core of **IV**.

Conclusions

The synthesis of multimetallic M/S clusters by the reductive coupling of dimeric building blocks appears to be of general utility. Under reducing conditions, dinuclear clusters with coordinatively unsaturated cores, such as $[Fe_2S_2]^{2+}$, $[MoFeS_2]^{4+}$ and $[MoFeSO]^{4+}$, couple to give cluster products with cores such as $[Fe_4S_4]^{2+}$, $[MoFe_3S_4]^{3+}$, $[MoFe_3S_3O]^{4+}$, $[Mo_2Fe_2S_4]^{4+}$ and $[MoFe_3S_4]^{2+}$. The synthesis of the $[Fe_4S_4]^{2+}$ cluster from the reductive coupling of $[Fe_2S_2]^{2+}$ has been previously reported [6]. However, the general utility of this coupling reaction in the synthesis of heterometallic clusters has not been thoroughly explored.

In this paper the reductive coupling approach has afforded clusters with the $[MoFe_3S_4]^{3+}$ and $[MoFe_3S_4]^{2+}$ cores. The reductive coupling synthesis of clusters with the $[Mo_2Fe_2S_4]^{4+}$ cores also has been achieved. The MoFe dimer and the Fe_2 dimer can be designated as A and B respectively. Using A and B as building blocks, clusters with a variety of core distributions such as A2 and AB have been obtained. The isolation in analytically pure form of all these clusters has been achieved. Product diversity is apparent and can be controlled by the use of appropriate ligands. All attempts to synthesize a cluster with an AB_3 core stoichiometry that would give a Mo/Fe/S composition closer to that of the FeMo cofactor of nitrogenase have been unsuccessful. Characteristically, the 1A:3B ratio reaction system under different conditions has been extensively explored but no cluster with a $MoFe_7S_8$ core could be obtained. In all cases, clusters with the A2B2, AB or B3, and A2 structural motifs were isolated. This synthetic system, however should be further explored because the synthesis of such a cluster is of paramount importance due to its relevance to the FeMoco cluster of nitrogenase. No cluster with a $MoFe_7$ has ever been synthesized.

This type of reductive coupling reactions combined with conditions that favor the removal of terminal ligands may be necessary for the synthesis of polynuclear clusters with a minimum of terminal ligands, and extensive bridging by core sulfido ligands, as found in the FeMoco of nitrogenase.Similar synthetic methodologies may also be applied for the synthesis of analogues for the P-clusters of nitrogenase.

Acknowledgments. We thank Dr. Jeff Campf for X-ray data collection. The authors acknowledge the support of this work by a grant from the National Institutes of Health (GM 33080).

References

[1] O. Einsle, A. F. Tezcan, S. L. A. Andrade, B. Schmid, M. Yoshida, J. B. Howard, D. C. Rees, *Science* **2002**, *297*, 1696−1700.

[2] (a) B. K. Burgess, D. J. Lowe, *Chem. Rev.* **1996**, *96*, 2983−3011; (b) J. B. Howard, D. C. Rees, *Chem. Rev.* **1996**, *96*, 2965−2982.

[3] (a) U. Huniar, R. Ahlrichs, D. Coucouvanis, *J. Am. Chem. Soc.* **2004**, *126*, 2588; (b) T. C. Yang, N. K. Maeser, M. Laryukhin, H. I. Lee, D. R. Dean, L. C. Seefeldt, B. M. Hoffman, *J. Am. Chem. Soc.* **2005**, *127*, 12804−1280; (c) B. Hinneman, J. K. Nórskov, *J. Am. Chem. Soc.* **2003**, *125*, 1466; (d) I. Dance, *Chem. Commun.* **2003**, 324−325; (e) T. Lovell, T. Liu, D. A. Case, L. Noodleman, *J. Am. Chem. Soc.* **2003**, 125, 8377−8383; (f) B. Hinnemann, K. Nórskov, *J. Am. Chem. Soc*. **2004**, 126, 3920−3927; (g) R. Y. Igarashi, L. C. Seefeldt, *Crit. Rev. Biochem. Mol. Biol.* **2003**, *38*, 351−384.

[4] (a) S. M. Malinak, D. Coucouvanis, *Prog. Inorg. Chem*. **2001**, *49*, 599 and references therein; (b) S. C. Lee, R. H.Holm, *Chem. Rev.* **2004**, *104*, 1135 and references therein.

[5] (a) K. D. Demadis, C. F. Campana, D. Coucouvanis, *J. Am. Chem. Soc.* **1995**, *117*, 7832; (b) F. Osterloh, B. M. Segal, C. Achim, R. H. Holm, *Inorg. Chem.* **2000**, *39*, 980.

[6] J. Han, M. Koutmos, S. Al-Ahmad, D. Coucouvanis, *Inorg. Chem*. **2001**, *40*, 5985−5999.

[7] J. W. McDonald, G. D. Frisen, L. D. Resenhein, W. E. Newton, *Inorg. Chim. Acta.* **1983**, *72*, 205.

[8] N. S. Gill, F. B. Taylor, *Inorg. Synth.* **1967**, *9*, 136.

[9] G. B. Wong, M. A. Bobrik, R. H. Holm, *Inorg. Chem.* **1978**, *17*, 578−584.

[10] D. J. Daigle, *Inorg. Synth.* **1998**, *32*, 40−45.

[11] G. M. Sheldrick, SADABS, v.2.10. Program for Empirical Absorption Correction of Area Detector Data, University of Göttingen, Göttingen, (Germany) **2003**.

[12] SHELXTL, v.6.10. Siemens Industrial Automation, Inc., Madison, WI, **2000**.

[13] C. A. Tolman, *Chem. Rev.* **1977**, *77*, 313−348.

[14] (a) D. Coucouvanis, J. Han, N. Moon, *J. Am. Chem. Soc.* **2002**, *124*, 216; (b) M. A. Tyson, D. Coucouvanis, *Inorg. Chem.* **1997**, *36*, 3808.

[15] (a) T. E. Wolff, J. M. Berg, R. H. Holm, *Inorg. Chem.* **1981**, *20*, 174−180; b) R. E. Palermo, R. H. Holm, *J. Am. Chem. Soc.* **1983**, *105*, 4310; c) K. D. Demadis, D. Coucouvanis, *Inorg. Chem.* **1995**, *34*, 436−448.

[16] (a) D. Coucouvanis, *Acc. Chem. Res.* **1981**, *14*, 201; (b) D. Coucouvanis, *Acc. Chem. Res.* **1991**, *24*, 1; (c) R. H. Holm, E. D. Simhon, In *Molybdenum Enzymes*; Spiro, T. G., Ed.; Wiley Interscience: New York, **1985**; pp 1−87.

[17] J.-Q. Xu, J.-S. Qian, Q. Wei, N.-H. Hu, Z.-S. Jin, G.-C. Wei, *Inorg. Chim. Acta.* **1989**, *164*, 55.

[18] H. Kawaguchi, K. Yamada, S. Ohnish, K. Tatsumi, *J. Am. Chem. Soc.* **1997**, *119*, 10871.

[19] M. A. Mansour, M. D. Curtis, J. W. Kampf, *Organometallics* **1997**, *16*, 275.

[20] H. Brunner, N. Janietz, J. Wachter, T. Zahn, M. Ziegler, *Angew. Chem. Int. Ed. Engl.* **1985**, *24*, 133.

